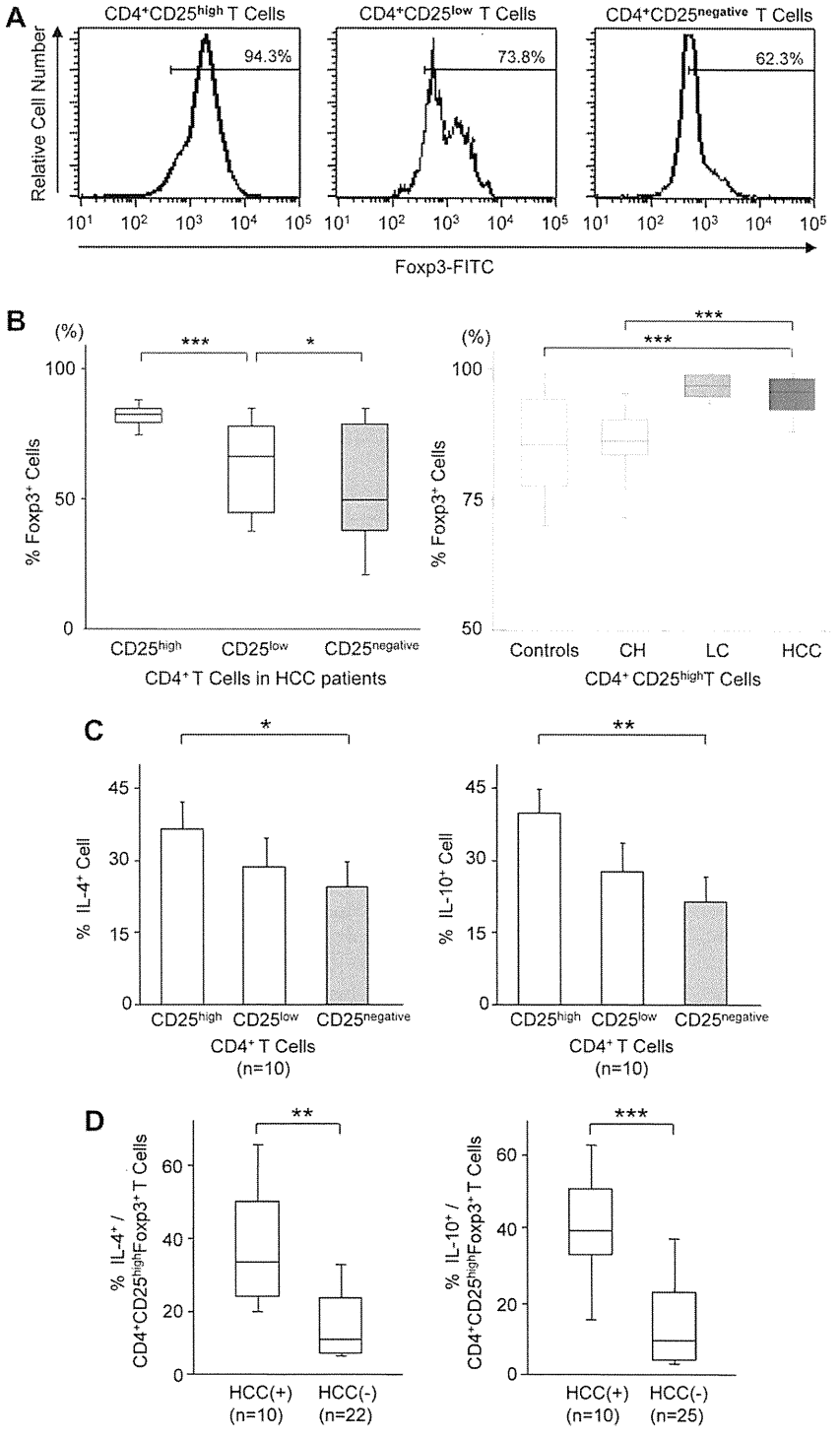

Fig. 2. Analysis of intracellular Foxp3 expression and cytokine production in $CD4^+$ $CD25^{high/low/negative}$ T cell subsets in HCC patients. (A) Representative expression of Foxp3 in $CD4^+$ T cells from an individual subject. Intracellular Foxp3 was stained following membrane permeabilization. Intracellular Foxp3 was detected by the specific mAb. (B) Statistical analysis in the left side panel shows that the percent of $Foxp3^+$ cells in the $CD4^+CD25^{high}$ T cell subset in HCC patients was significantly larger than that of $CD4^+CD25^{low/negative}$ T cell subsets, and in the right side panel shows that that of $CD4^+CD25^{high}$ T cell subset in HCC patients was significantly larger than that of $CD4^+CD25^{high}$ T cells in healthy controls and CH patients. (C) Statistical analysis shows that the levels of Th2 cytokines IL-4 and IL-10 were remarkably high in the $CD4^+CD25^{high}$ T cell subset. (D) Comparison of intracellular cytokine production in $CD4^+CD25^{high}$ T cell subsets between patients with and without HCC. Healthy controls, patients with chronic hepatitis and liver cirrhosis were included in the HCC (−) column. IL-4 and IL-10 levels were higher in the $CD4^+CD25^{high}$ T cell subset in HCC patients. *Indicates $P < 0.05$, **indicates $P < 0.01$ and ***indicates $P < 0.001$.

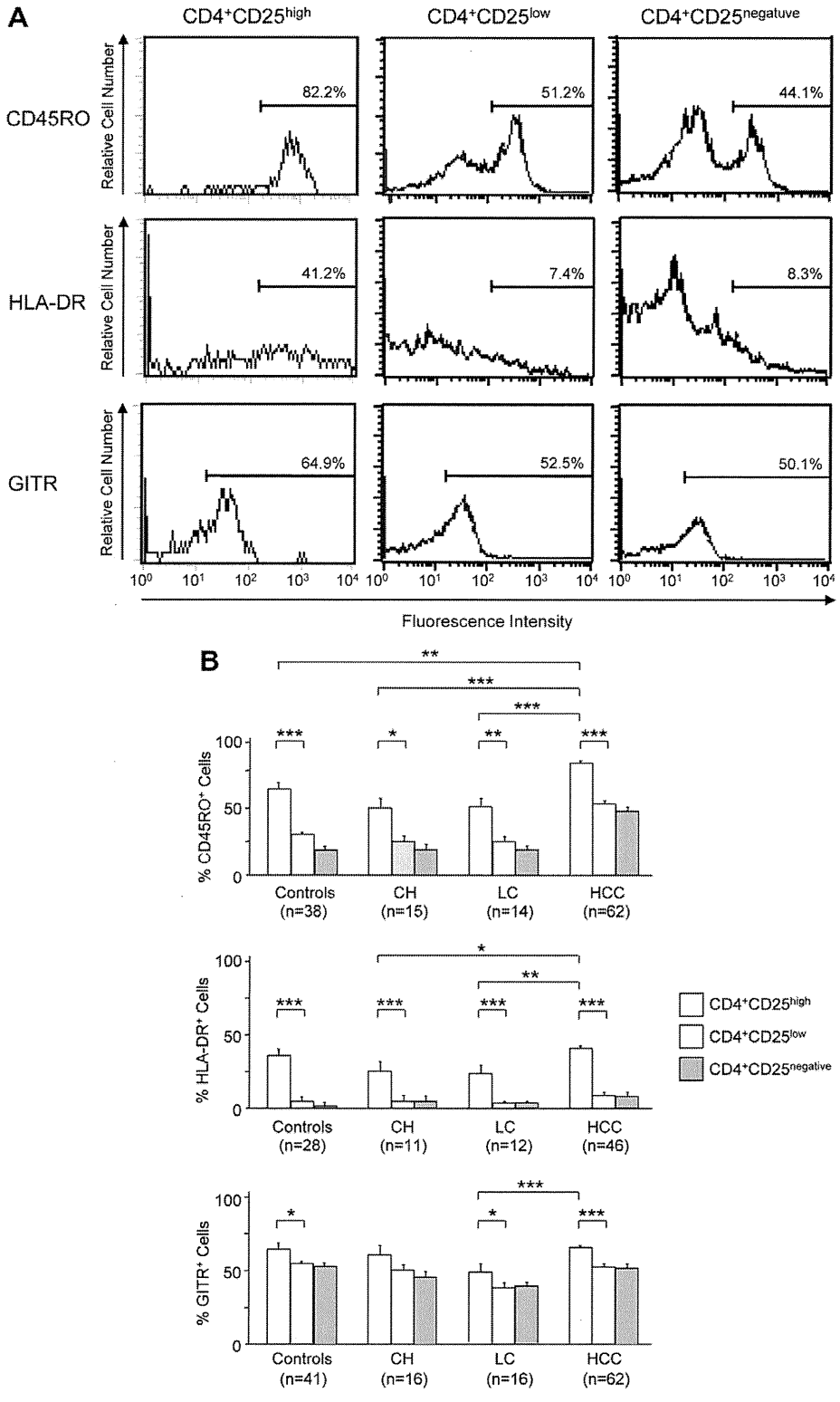

Fig. 3. Phenotypic analysis of $CD4^+CD25^{high/low/negative}$ T cell subsets in HCC patients. Fleshly isolated $CD4^+$ T cells (at least 2×10^5 cells/tube) from HCC patients were labeled with anti-CD4, anti-CD25, anti-CD45RA, anti-CD45RO, anti-CD62L, anti-CCR7, anti-CTLA-4, anti-HLA-DR and anti-GITR mAbs. (A) Representative CD45RO, HLA-DR, and GITR expression profiles in $CD4^+$ T cell subsets that differ in CD25 expression. (B) Statistical analysis shows that the proportions of $CD45RO^+$, $HLA\text{-}DR^+$ and $GITR^+$ were elevated in the $CD4^+CD25^{high}$ T cell subsets of all patient groups compared to the $CD4^+CD25^{low/negative}$ T cell subsets, except for $GITR^+$ cells in CH patients ($P < 0.05$). The percentage of $CD45RO^+$ cells in HCC patients was elevated compared to the patients with advanced liver diseases and healthy controls. *Indicates $P < 0.05$, **indicates $P < 0.01$ and ***indicates $P < 0.001$.

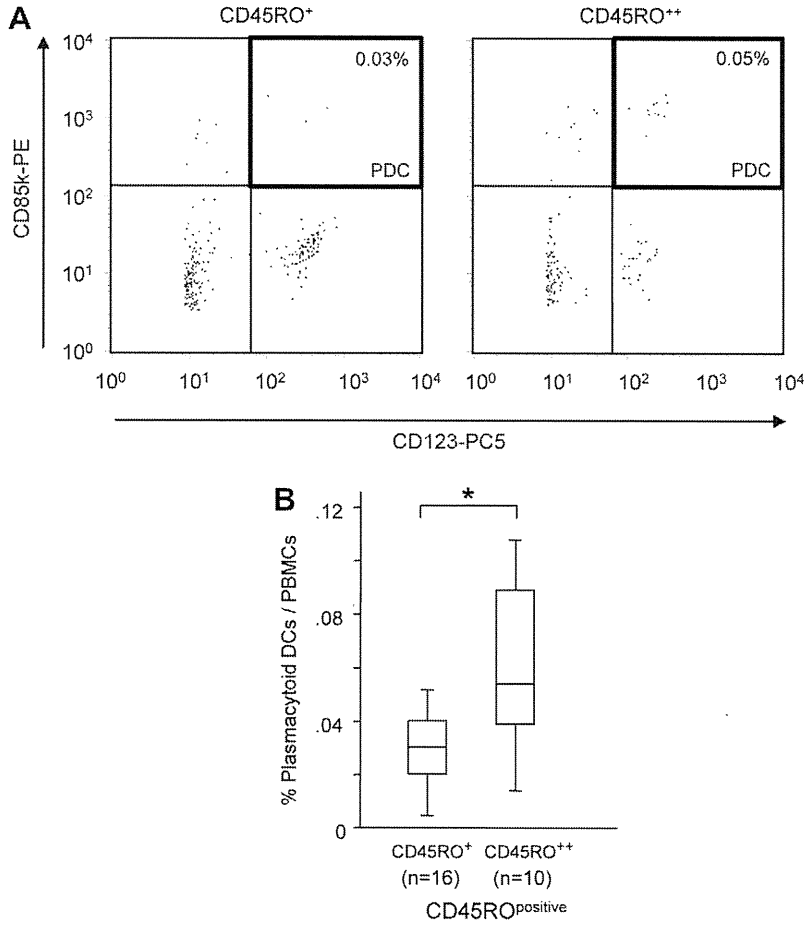

Fig. 4. Frequencies of plasmacytoid DCs in peripheral blood of HCC patients. Whole blood cells were analyzed by flow cytometry following staining with a combination of the mAbs. HCC patients were divided into two groups according to the frequencies of $CD45RO^{positivee}$ cells in $CD4^+CD25^{high}$ T cell subset ($CD45RO^+$ vs. $CD45RO^{++}$). Patients with $CD45RO^{++}$ contained > 83.8% positive cells in $CD4^+CD25^{high}$ T cells. (A) Representative dot plots of plasmacytoid DCs. Plasmacytoid DCs of $CD45RO^+$ group are shown in the left panel and $CD45RO^{++}$ group in the right panel. (B) Statistical analysis shows that the frequencies of plasmacytoid DCs were significantly higher in $CD45RO^{++}$ group. *Indicates $P < 0.05$.

and fibrosis stages between two groups as described above. The levels of serum AFP and DCP and the maximum tumor diameters in $CD45RO^{++}$ group were larger than those in $CD45RO^+$ group (Fig. 4). Others were not significantly different between two groups. These results imply that a subset of Tregs may contribute to the progression of liver tumors.

4. Discussion

$CD4^+CD25^{high}$ $Foxp3^+$ regulatory T cells have been shown to increase in patients with malignancies to suppress the immune responses. In this study, we provide evidence that patients with HCC have increased frequencies of $CD4^+CD25^{high}$ T cells in their peripheral blood compared to healthy controls and chronic hepatitis patients. A large proportion of $CD4^+CD25^{high}$ T cells expressed Foxp3 and produced Th2 cytokines. We also showed that $CD4^+CD25^{high}$ T cells expressed high levels of CD45RO, HLA-DR and GITR, and, interestingly, the T cell frequencies expressing these surface molecules were associated with plasmacytoid DC numbers and maximum tumor diameters in HCC patients.

There are several reports of elevated numbers of Treg cells in the peripheral blood and tumor tissues of patients with different types of cancer [3–12]. The study of Unitt et al. provided the first report of increased $CD4^+CD25^+$ T cell frequency within tumor tissue compared to non-tumor tissue in HCC patients [13]. Ormandy et al. showed that the frequency of $CD4^+CD25^{high}$ T cells in peripheral blood of patients with HCC was significantly higher (3.92 ± 3.3%) than in healthy donors (1.17 ± 0.87%) and liver cirrhosis patients (0.78 ± 0.43%) [3]. Our data revealed that a minimal increase in $CD4^+CD25^{high}$ T cells was detected in LC patients and more pronounced changes were found in HCC patients.

We showed that higher percentages of $CD4^+CD25^{high}$ T cells produced Th2 cytokines IL-4 and IL-10 in HCC patients. Tregs were recently observed to produce IL-10 [25–27], which can be a major mediator of immune suppression [28–30]. Voo et al. reported that Tregs in the peripheral blood of healthy donors secreted IL-10 but not IL-2, IFN-γ, or IL-4 [31]. Schmitz-Winnenthal et al. demon-

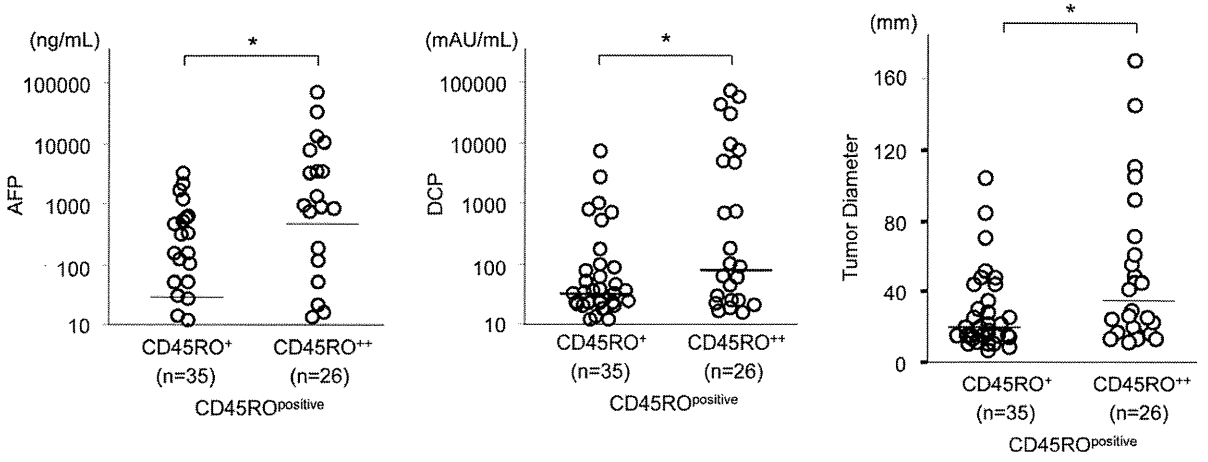

Fig. 5. Prevalence of $CD4^+CD25^{high/low/negative}$ T cell subsets and tumor progression. The levels of AFP and DCP and the maximum tumor diameters in $CD45RO^{++}$ group were larger than those in $CD45RO^+$ groups. AFP, alpha-fetoprotein; DCP, des-gamma-carboxyl prothrombin. *Indicates $P < 0.05$.

strated the presence of Treg secreting IL-10 but not IL-4 or IFN-γ upon antigen recognition in chronic pancreatitis patients [32]. The present data demonstrated that larger numbers of Tregs produced not only IL-10 but also IL-4 in HCC patients, which may contribute to the strong immunosuppressive properties of the T cells in liver malignancies.

It appears that Tregs consists of heterogenous populations within $CD4^+$ T cells, and that a subset of $CD4^+CD25^{high}$ T cells could be subdivided into different functional subsets based on the expression of various surface molecules [6]. The proportions of Tregs expressing these molecules are reported to be different in the various forms of cancer. The prevalence of $CD45RO^+$ and $GITR^+$ Treg cells is higher in $CD4^+CD25^{high}$ T cells than in $CD4^+CD25^{low/negative}$ T cells in renal cell carcinoma [4]. In head and neck squamous cell carcinoma, however, $CD4^+CD25^{high}$ T cells express CTLA-4, Foxp3, and CD62L but little GITR, and $CD25^{low/negative}$ T cells express intermediate to high levels of GITR and HLA-DR [8]. Our study showed that Tregs in HCC patients expressed significantly higher levels of CD45RO, HLA-DR and GITR compared to $CD4^+CD25^{low/negative}$ cells, suggesting that the activated populations of Tregs may contribute to the establishment of immunosuppressive microenvironments.

Little is known about the molecular and cellular mechanisms responsible for the increase and maintenance of elevated numbers of Treg cells in cancer. DCs have pivotal roles in the induction of tolerogenic/regulatory T cells [20,33]. In peripheral blood, there are two distinct populations of DCs which can be distinguished based on phenotypical and morphological characteristics; myeloid DCs (mDCs) and plasmacytoid DCs (pDCs) [18,34]. Our data demonstrated that higher frequencies of $CD45RO^+CD4^+CD25^{high}$ T cells were associated with higher frequencies of pDCs in the peripheral blood of HCC patients. When the tumor antigens are assumed by pDCs through Toll-like receptor 9 (TLR9) via receptor-mediated endocytosis, secretions of pro-inflammatory cytokines, such as type I interferons (IFNs), would be caused. On the contrary, pDC may regulate anti-tumor immunity and support immune evasion and tumor escape. They exhibit reduced IFN-α production upon TLR9 stimulation and can induce IL-10 producing $CD4^+$ and $CD8^+$ Treg [35,36]. This suggests that anti-tumor immune responses can be regulated through both modulation of pDC function by the tumor and by limiting anti-tumor cytolytic activity through induction of $CD8^+$ Treg.

Concerning the association of Tregs and prognosis, it has been reported that an increased number of circulating Tregs predicts poor survival of patients with renal cell carcinoma [4], gastric and esophageal cancers [7], myelodysplastic syndrome [37] and HCC [11]. In addition, tumor-infiltrating Tregs were associated with reduced survival in ovarian cancer [12] and HCC patients [1]. In addition, we found that $CD45RO^+CD4^+CD25^{high}$ T cell subset was associated with larger tumor burdens, implying that a subset of Tregs may contribute to the promotion of tumor cell growth in the liver. However, it is also well possible that this just reflects stronger activation caused by a larger amount of antigen.

We performed the functional evaluation of Tregs derived from HCC patients by incubating with responder $CD4^+CD25^-$ T cells (Tresp). We observed that $CD45RO^+$ $CD4^+CD25^{high}$ T cells of HCC patients did not suppress the proliferation of responder T cells when co-cultured at Treg/Tresp ratios of 1:2 and 1:8 (data not shown). In contrast, Hoffmann et al. confirmed that the $CD45RA^+$ $CD4^+CD25^{high}$ T cells of healthy volunteers give rise to a homogeneous and highly suppressive Treg cell population, whereas $CD45RA\text{-}CD4^+CD25^{high}$ T cells generate cell lines with mixed phenotype and function [38]. Although the reasons of these conflicting data were not clarified in the current study, cell viability, apoptosis susceptibility, involvement of Th1 cytokines, and interaction to helper T cell subsets of Tregs obtained from HCC patients need to be evaluated in the future experiments.

This study may be helpful for a better characterization of Treg subsets in the peripheral circulation of patients with HCC, which may establish the immunosuppressive environment to promote tumor progression. Furthermore, to gain insights into changes in the Treg subsets

during the therapeutic option may lead to more effective immunotherapies against cancer and may improve prognosis.

Conflict of interest

None declared.

Acknowledgements

We thank Ms. Mariko Katsuda for technical assistance. We also thank the patients for participating in this study.

References

[1] J. Zhou, T. Ding, W. Pan, L.Y. Zhu, L. Li, L. Zheng, Increased intratumoral regulatory T cells are related to intratumoral macrophages and poor prognosis in hepatocellular carcinoma patients, Int. J. Cancer 125 (2009) 1640–1648.
[2] Y. Nakamoto, E. Mizukoshi, H. Tsuji, Y. Sakai, M. Kitahara, K. Arai, T. Yamashita, K. Yokoyama, N. Mukaida, K. Matsushima, O. Matsui, S. Kaneko, Combined therapy of transcatheter hepatic arterial embolization with intratumoral dendritic cell infusion for hepatocellular carcinoma: clinical safety, Clin. Exp. Immunol. 147 (2007) 296–305.
[3] L.A. Ormandy, T. Hillemann, H. Wedemeyer, M.P. Manns, T.F. Greten, F. Korangy, Increased populations of regulatory T cells in peripheral blood of patients with hepatocellular carcinoma, Cancer Res. 65 (2005) 2457–2464.
[4] R.W. Griffiths, E. Elkord, D.E. Gilham, V. Ramani, N. Clarke, P.L. Stern, R.E. Hawkins, Frequency of regulatory T cells in renal cell carcinoma patients and investigation of correlation with survival, Cancer Immunol. Immunother. 56 (2007) 1743–1753.
[5] J. Visser, H.W. Nijman, B.N. Hoogenboom, P. Jager, D. van Baarle, E. Schuuring, W. Abdulahad, F. Miedema, A.G. van der Zee, T. Daemen, Frequencies and role of regulatory T cells in patients with (pre)malignant cervical neoplasia, Clin. Exp. Immunol. 150 (2007) 199–209.
[6] C. Schaefer, G.G. Kim, A. Albers, K. Hoermann, E.N. Myers, T.L. Whiteside, Characteristics of CD4+CD25+ regulatory T cells in the peripheral circulation of patients with head and neck cancer, Br. J. Cancer 92 (2005) 913–920.
[7] K. Kono, H. Kawaida, A. Takahashi, H. Sugai, K. Mimura, N. Miyagawa, H. Omata, H. Fujii, CD4(+)CD25 high regulatory T cells increase with tumor stage in patients with gastric and esophageal cancers, Cancer Immunol. Immunother. 55 (2006) 1064–1071.
[8] L. Strauss, C. Bergmann, W. Gooding, J.T. Johnson, T.L. Whiteside, The frequency and suppressor function of CD4+CD25highFoxp3+ T cells in the circulation of patients with squamous cell carcinoma of the head and neck, Clin. Cancer Res. 13 (2007) 6301–6311.
[9] A.M. Wolf, D. Wolf, M. Steurer, G. Gastl, E. Gunsilius, B. Grubeck-Loebenstein, Increase of regulatory T cells in the peripheral blood of cancer patients, Clin. Cancer Res. 9 (2003) 606–612.
[10] F. Ichihara, K. Kono, A. Takahashi, H. Kawaida, H. Sugai, H. Fujii, Increased populations of regulatory T cells in peripheral blood and tumor-infiltrating lymphocytes in patients with gastric and esophageal cancers, Clin. Cancer Res. 9 (2003) 4404–4408.
[11] J. Fu, D. Xu, Z. Liu, M. Shi, P. Zhao, B. Fu, Z. Zhang, H. Yang, H. Zhang, C. Zhou, J. Yao, L. Jin, H. Wang, Y. Yang, Y.X. Fu, F.S. Wang, Increased regulatory T cells correlate with CD8 T-cell impairment and poor survival in hepatocellular carcinoma patients, Gastroenterology 132 (2007) 2328–2339.
[12] T.J. Curiel, G. Coukos, L. Zou, X. Alvarez, P. Cheng, P. Mottram, M. Evdemon-Hogan, J.R. Conejo-Garcia, L. Zhang, M. Burow, Y. Zhu, S. Wei, I. Kryczek, B. Daniel, A. Gordon, L. Myers, A. Lackner, M.L. Disis, K.L. Knutson, L. Chen, W. Zou, Specific recruitment of regulatory T cells in ovarian carcinoma fosters immune privilege and predicts reduced survival, Nat. Med. 10 (2004) 942–949.
[13] E. Unitt, S.M. Rushbrook, A. Marshall, S. Davies, P. Gibbs, L.S. Morris, N. Coleman, G.J. Alexander, Compromised lymphocytes infiltrate hepatocellular carcinoma: the role of T-regulatory cells, Hepatology 41 (2005) 722–730.
[14] E. Biagi, I. Di Biaso, V. Leoni, G. Gaipa, V. Rossi, C. Bugarin, G. Renoldi, M. Parma, A. Balduzzi, P. Perseghin, A. Biondi, Extracorporeal photochemotherapy is accompanied by increasing levels of circulating CD4+CD25+GITR+Foxp3+CD62L+ functional regulatory T-cells in patients with graft-versus-host disease, Transplantation 84 (2007) 31–39.
[15] J.N. Stoop, R.G. van der Molen, C.C. Baan, L.J. van der Laan, E.J. Kuipers, J.G. Kusters, H.L. Janssen, Regulatory T cells contribute to the impaired immune response in patients with chronic hepatitis B virus infection, Hepatology 41 (2005) 771–778.
[16] R.W. van Olffen, N. Koning, K.P. van Gisbergen, F.M. Wensveen, R.M. Hoek, L. Boon, J. Hamann, R.A. van Lier, M.A. Nolte, GITR triggering induces expansion of both effector and regulatory CD4+ T cells in vivo, J. Immunol. 182 (2009) 7490–7500.
[17] B. Wilde, S. Dolff, X. Cai, C. Specker, J. Becker, M. Totsch, U. Costabel, J. Durig, A. Kribben, J.W. Tervaert, K.W. Schmid, O. Witzke, CD4+CD25+ T-cell populations expressing CD134 and GITR are associated with disease activity in patients with Wegener's granulomatosis, Nephrol. Dial. Transplant 24 (2009) 161–171.
[18] J.S. Ahn, D.K. Krishnadas, B. Agrawal, Dendritic cells partially abrogate the regulatory activity of CD4+CD25+ T cells present in the human peripheral blood, Int. Immunol. 19 (2007) 227–237.
[19] Q. Tang, J.A. Bluestone, Plasmacytoid DCs and T(reg) cells: casual acquaintance or monogamous relationship?, Nat Immunol. 7 (2006) 551–553.
[20] I.E. Dumitriu, D.R. Dunbar, S.E. Howie, T. Sethi, C.D. Gregory, Human dendritic cells produce TGF-beta 1 under the influence of lung carcinoma cells and prime the differentiation of CD4+CD25+Foxp3+ regulatory T cells, J. Immunol. 182 (2009) 2795–2807.
[21] J. Bayry, F. Triebel, S.V. Kaveri, D.F. Tough, Human dendritic cells acquire a semimature phenotype and lymph node homing potential through interaction with CD4+CD25+ regulatory T cells, J. Immunol. 178 (2007) 4184–4193.
[22] S. Hori, T. Nomura, S. Sakaguchi, Control of regulatory T cell development by the transcription factor Foxp3, Science 299 (2003) 1057–1061.
[23] H. Yagi, T. Nomura, K. Nakamura, S. Yamazaki, T. Kitawaki, S. Hori, M. Maeda, M. Onodera, T. Uchiyama, S. Fujii, S. Sakaguchi, Crucial role of FOXP3 in the development and function of human CD25+CD4+ regulatory T cells, Int. Immunol. 16 (2004) 1643–1656.
[24] J.D. Fontenot, M.A. Gavin, A.Y. Rudensky, Foxp3 programs the development and function of CD4+CD25+ regulatory T cells, Nat. Immunol. 4 (2003) 330–336.
[25] C.L. Maynard, L.E. Harrington, K.M. Janowski, J.R. Oliver, C.L. Zindl, A.Y. Rudensky, C.T. Weaver, Regulatory T cells expressing interleukin 10 develop from Foxp3+ and Foxp3-precursor cells in the absence of interleukin 10, Nat. Immunol. 8 (2007) 931–941.
[26] C.M. Freeman, B.C. Chiu, V.R. Stolberg, J. Hu, K. Zeibecoglou, N.W. Lukacs, S.A. Lira, S.L. Kunkel, S.W. Chensue, CCR8 is expressed by antigen-elicited, IL-10-producing CD4+CD25+ T cells, which regulate Th2-mediated granuloma formation in mice, J. Immunol. 174 (2005) 1962–1970.
[27] H.H. Uhlig, J. Coombes, C. Mottet, A. Izcue, C. Thompson, A. Fanger, A. Tannapfel, J.D. Fontenot, F. Ramsdell, F. Powrie, Characterization of Foxp3+CD4+CD25+ and IL-10-secreting CD4+CD25+ T cells during cure of colitis, J. Immunol. 177 (2006) 5852–5860.
[28] A. Wakkach, S. Augier, J.P. Breittmayer, C. Blin-Wakkach, G.F. Carle, Characterization of IL-10-secreting T cells derived from regulatory CD4+CD25+ cells by the TIRC7 surface marker, J. Immunol. 180 (2008) 6054–6063.
[29] M. Torisu, H. Murakami, F. Akbar, H. Matsui, Y. Hiasa, B. Matsuura, M. Onji, Protective role of interleukin-10-producing regulatory dendritic cells against murine autoimmune gastritis, J. Gastroenterol. 43 (2008) 100–107.
[30] M. Bettini, D.A. Vignali, Regulatory T cells and inhibitory cytokines in autoimmunity, Curr. Opin. Immunol. 21 (2009) 612–618.
[31] K.S. Voo, Y.H. Wang, F.R. Santori, C. Boggiano, K. Arima, L. Bover, S. Hanabuchi, J. Khalili, E. Marinova, B. Zheng, D.R. Littman, Y.J. Liu, Identification of IL-17-producing FOXP3+ regulatory T cells in humans, Proc. Natl. Acad. Sci. USA 106 (2009) 4793–4798.
[32] H. Schmitz-Winnenthal, D.H. Pietsch, S. Schimmack, A. Bonertz, F. Udonta, Y. Ge, L. Galindo, S. Specht, C. Volk, K. Zgraggen, M. Koch, M.W. Buchler, J. Weitz, P. Beckhove, Chronic pancreatitis is associated with disease-specific regulatory T-cell responses, Gastroenterology 138 (2010) 1178–1188.
[33] B. Eksteen, J.M. Neuberger, Mechanisms of disease: the evolving understanding of liver allograft rejection, Nat. Clin. Pract. Gastroenterol. Hepatol. 5 (2008) 209–219.
[34] Shiina, K. Kobayashi, T. Kobayashi, Y. Kondo, Y. Ueno, T. Shimosegawa, Dynamics of immature subsets of dendritic cells during antiviral therapy in HLA-A24-positive chronic hepatitis C patients, J. Gastroenterol. 41 (2006) 758–764.

[35] J. Charles, J. Di Domizio, D. Salameire, N. Bendriss-Vermare, C. Aspord, R. Muhammad, C. Lefebvre, J. Plumas, M.T. Leccia, L. Chaperot, Characterization of circulating dendritic cells in melanoma: role of CCR6 in plasmacytoid dendritic cell recruitment to the tumor, J. Invest. Dermatol. 130 (2010) 646–656.
[36] S. Wei, I. Kryczek, L. Zou, B. Daniel, P. Cheng, P. Mottram, T. Curiel, A. Lang, W. Zou, Plasmacytoid dendritic cells induce CD8+ regulatory T cells in human ovarian carcinoma, Cancer Res. 65 (2005) 5020–5026.
[37] S.Y. Kordasti, W. Ingram, J. Hayden, D. Darling, L. Barber, B. Afzali, G. Lombardi, M.W. Wlodarski, J.P. Maciejewski, F. Farzaneh, G.J. Mufti, CD4+CD25high Foxp3+ regulatory T cells in myelodysplastic syndrome (MDS), Blood 110 (2007) 847–850.
[38] P. Hoffmann, R. Eder, T.J. Boeld, K. Doser, B. Piseshka, R. Andreesen, M. Edinger, Only the CD45RA+ subpopulation of CD4+CD25high T cells gives rise to homogeneous regulatory T-cell lines upon in vitro expansion, Blood 108 (2006) 4260–4267.

Note: This copy is for your personal, non-commercial use only. To order presentation-ready copies for distribution to your colleagues or clients, contact us at *www.rsna.org/rsnarights.*

Liver Fibrosis in Patients with Chronic Hepatitis C: Noninvasive Diagnosis by Means of Real-time Tissue Elastography—Establishment of the Method for Measurement[1]

Yohei Koizumi, MD
Masashi Hirooka, MD, PhD
Yoshiyasu Kisaka, MD, PhD
Ichiro Konishi, MD, PhD
Masanori Abe, MD, PhD
Hidehiro Murakami, MD, PhD
Bunzo Matsuura, MD, PhD
Yoichi Hiasa, MD, PhD
Morikazu Onji, MD, PhD

Purpose: To prospectively measure liver stiffness with real-time tissue elastography in patients with chronic hepatitis C and to compare the results with those of clinical assessment of fibrosis by using histologic stage as the reference standard.

Materials and Methods: All subjects gave informed consent, and the study was approved by the institutional ethics committee. Seventy hospitalized patients (46 men, 24 women; mean age, 65.5 years ± 11.7 [standard deviation]; age range, 33–87 years) with chronic hepatitis C underwent real-time elastography between January 2009 and September 2009. Elastography was performed at four liver locations by two independent observers. The elastic ratio (ratio of the value in the intrahepatic venous small vessels divided by the value in the hepatic parenchyma) was calculated and was compared with histologic fibrosis stage at liver biopsy. The elastic ratio and clinical fibrosis markers were assessed by using receiver operating characteristic (ROC) analysis. The differences between body site and observers were assessed with κ statistics and intraclass correlation coefficients (ICCs).

Results: Real-time tissue elastography cutoff values were 2.73 for F of 2 or greater, 3.25 for F of 3 or greater, and 3.93 for F of 4. No site differences were observed (κ = 0.835, ICC = 0.966), and the elastic ratio measurement was correlated between the two examiners (r^2 = 0.869, $P < .0001$). The areas under the ROC curves for elastic ratio, hyaluronic acid, type IV collagen, aspartate aminotransferase–to–platelet ratio index, FibroIndex, Forns score, and Hepascore were 0.95, 0.32, 0.73, 0.76, 0.76, 0.87, and 0.70, respectively; the elastic ratio performed better than the serum fibrosis markers and other scores.

Conclusion: Real-time tissue elastography is not invasive and could be used to evaluate liver fibrosis in patients with chronic hepatitis C.

©RSNA, 2011

Supplemental material: *http://radiology.rsna.org/lookup/suppl/doi:10.1148/radiol.10100319/-/DC1*

[1] From the Department of Gastroenterology and Metabology, Ehime University Graduate School of Medicine, Shitsukawa, Toon, Ehime 791-0295, Japan. Received February 9, 2010; revision requested March 24; revision received June 22; accepted July 13; final version accepted August 11. Supported by a Grant-in-Aid for Scientific Research (C) (Japan Society for the Promotion of Science, KAKENHI 21590848) and the Program for Enhancing Systematic Education in Graduate School from the Ministry of Education, Culture, Sports, Science and Technology, Tokyo, Japan. **Address correspondence to** Y.H. (e-mail: *hiasa@m.ehime-u.ac.jp*).

©RSNA, 2011

Chronic viral hepatitis infection increases liver fibrosis and stiffness and is an important cause of liver cirrhosis (1). Although liver biopsy is the reference standard for the diagnosis of liver fibrosis (2), it is an invasive procedure, which is difficult to perform in patients who need to be examined repeatedly to monitor the progression of liver fibrosis. Moreover, the evaluation of fibrosis with liver biopsy is associated with adverse events (3), sampling errors (4,5), and interpathologist and intrapathologist variabilities (6). Therefore, many studies have evaluated other noninvasive methods, such as the use of sonographic transient elastography (FibroScan; EchoSens, London, England) (7) and acoustic radiation force impulse (8) and laboratory tests, such as the aspartate aminotransferase-to-platelet ratio index, the FibroIndex, the Forns score, and the Hepascore, for the assessment of liver fibrosis stage.

Transient elastography is one of the techniques that can be used to evaluate mean tissue stiffness noninvasively (7). Results of several recent studies (9) have shown that measurements of liver stiffness with transient elastography are well correlated with fibrosis METAVIR stages. In addition, transient elastography is advantageous in that it can be repeatedly performed, does not require a highly experienced operator, and has a low risk of complications. However, there is a problem with reproducibility at identical measurement positions (10). In addition, it is not a real-time technique, because the image is not visible while the measurement is being taken. The reproducibility of transient elastography is also substantially reduced in patients with steatosis and increased body mass index (BMI) because the modality of ultrasonography (US) itself has limitations for visualizing the liver clearly in such patients (11).

Real-time tissue elastography is a relatively new method for the measurement of tissue elasticity. It uses a B-mode US machine, incorporating elastography into the conventional US scanner (12). In the previously reported technique, a US probe is used to slightly compress or relax the body (13), and the echo signals are captured in real time. This device calculates the relative hardness of tissue and displays this information as real-time color images (14); it can display tissue elasticity images and conventional B-mode images at the same time.

The purpose of this prospective study was to measure liver stiffness with real-time elastography in patients with chronic hepatitis C and to compare the results with those of other clinical assessments of fibrosis by using the histologic stage of fibrosis as the reference standard.

Advances in Knowledge

- In patients with hepatitis C, the areas under the receiver operating characteristic curves for prediction of fibrosis by means of elastic ratio, hyaluronic acid level, type IV collagen level, aspartate aminotransferase-to-platelet ratio index, FibroIndex, Forns score, and Hepascore were 0.95, 0.32, 0.73, 0.76, 0.76, 0.87, and 0.70, respectively, indicating that the elastic ratio performed better than the other serum fibrosis markers and scores.
- For METAVIR stages identified at histologic examination, real-time elastography cutoff values were 2.73 for F of 2 or greater, 3.25 for F of 3 or greater, and 3.93 for F of 4.
- Our results were independent of observer ($r^2 = 0.869$, $P < .0001$) and measurement positioning site (intraclass correlation coefficient: 0.966, $\kappa = 0.835$).

Implications for Patient Care

- Real-time elastography is not invasive and could be used to repeatedly evaluate liver fibrosis.
- Real-time elastography could be a powerful tool for time-course evaluation of liver cirrhosis during antiviral therapy.

Materials and Methods

Patients

The study protocol was approved by the institutional review board, and written informed consent was obtained. All enrolled patients underwent liver biopsy as part of the study. Seventy patients with chronic hepatitis C (mean age, 65.5 years ± 11.7 [standard deviation]; range, 33–87 years) were hospitalized in the Department of Gastroenterology and Metabology, Ehime University Hospital, Japan, from January 2009 to September 2009, and liver stiffness, which is related to the grade of liver fibrosis, was measured. Of the 70 patients, 46 were men (mean age, 63.5 years ± 13.9; range, 33–87 years), and 24 were women (mean age, 66.6 years ± 10.3; range, 46–84 years).

Inclusion criteria were the presence of hepatitis C virus (HCV) ribonucleic acid in serum according to real-time polymerase chain reaction and positive HCV antibody. The exclusion criteria were ascites (because that might interfere with measurements), coinfection with other viruses such as hepatitis B virus, other liver diseases such as primary biliary

Published online
10.1148/radiol.10100319

Radiology 2011; 258:610–617

Abbreviations:
AUC = area under the ROC curve
BMI = body mass index
CI = confidence interval
ICC = intraclass correlation coefficient
ROC = receiver operating characteristic
ROI = region of interest

Author contributions:
Guarantors of integrity of entire study, Y. Koizumi, M.H., Y. Kisaka, I.K., M.A., B.M., Y.H., M.O.; study concepts/study design or data acquisition or data analysis/interpretation, all authors; manuscript drafting or manuscript revision for important intellectual content, all authors; manuscript final version approval, all authors; literature research, Y. Koizumi, M.H., Y. Kisaka, I.K., M.A., B.M., Y.H.; clinical studies, Y. Koizumi, M.H., Y. Kisaka, I.K., M.A., H.M., B.M., Y.H.; experimental studies, Y. Koizumi, M.H., Y. Kisaka, I.K., M.A., Y.H.; statistical analysis, Y. Koizumi, M.H., Y. Kisaka, I.K., M.A., Y.H.; and manuscript editing, Y. Koizumi, M.H., Y. Kisaka, I.K., M.A., B.M., Y.H., M.O.

Authors stated no financial relationship to disclose.

Figure 1

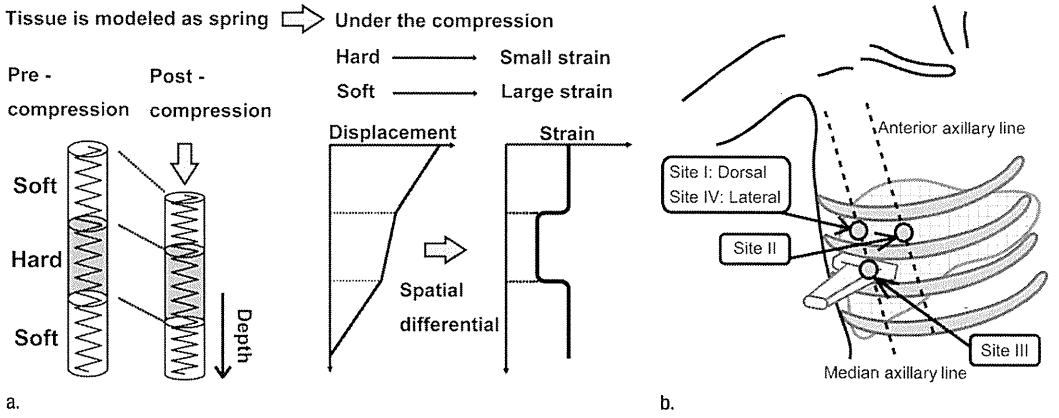

Figure 1: **(a)** The underlying method of real-time tissue elastography is the measurement and imaging of the strain distribution by adding the static pressure from the body surface; this is illustrated as a spring model. **(b)** The four measurement sites for real-time tissue elastography.

cirrhosis, and excessive alcohol consumption. (So that we could compare the METAVIR stages, which grade liver fibrosis only in patients with hepatitis C).

BMI and skin fold thickness were measured to determine whether they had any effects on real-time tissue elastography measurements.

Method for Measurement of Liver Stiffness

The underlining principle of real-time tissue elastography is illustrated in Figure 1a by using a spring model. When a spring is compressed, displacement in each section of the spring depends on the stiffness of the spring: A soft spring compresses more than a hard spring. The strain distribution, and in turn the stiffness in the spring, is measured by spatially differentiating the displacement at each location. On the basis of a previous report (13), we believed that compressing and relaxing the tissue with the US probe would be needed to measure the stiffness. However, we determined that we could measure the liver stiffness without adding any pressure from the probe because the liver itself receives pressure from the heartbeat automatically. Reflected US echoes are then used to compute the displacement and, thus, the strain distribution in the tissue. The examiners measured liver stiffness at four sites (Fig 1b), using the same positioning sites of the body as Boursier et al (10). The measurement sites were defined as follows: Site I was the dorsal decubitus and on the median axillary line and the first intercostal space; site II, the dorsal decubitus and on the anterior axillary line and the first intercostal space; site III, the dorsal decubitus and on the median axillary line and the second intercostal space; and site IV, the lateral decubitus and on the median axillary line and the first intercostal space. Real-time tissue elastography was performed five times at four measurement sites by two observers for each patient, in exhalation or inspiration to ensure that the liver was adequately depicted. The mean of the five measurements was calculated for comparison with histologic results.

Elastic Ratio

Hepatic elasticity was measured by using a US scanner with real-time tissue elastography (EUB-7500; Hitachi Medical Systems, Tokyo, Japan). We used a linear probe (EUP-L52; central frequency, 5.5 MHz). This scanner displays the color-coded elastography image overlaid on the B-mode image in real time (Fig 2a). Because this displayed color-coded elastography image shows only the relative tissue stiffness, a quantitative measuring technique called the elastic ratio was utilized.

The elastic ratio is the ratio of strain distribution in two selected regions of interest (ROIs). First, it was important to identify whether the hepatic vein or the portal vein would be a better internal control. We measured the value in the hepatic vein and portal vein for all 70 enrolled patients. The ROC curves of the elastic ratio calculated by using the ROI of the hepatic vein and the ROI of the portal vein as internal controls are shown in Figure 2b. The areas under the ROC curves (AUCs) of the elastic ratios obtained by using the hepatic vein as an internal control were higher than those obtained by using the portal vein as an internal control (intraclass correlation coefficient [ICC]: 0.953 [95% confidence interval {CI}: 0.903, 0.998] vs 0.731 [95% CI: 0.649, 0.886]; $P = .0006$). On the basis of the AUCs, the hepatic veins were used as an internal control. The ROI was placed on intrahepatic venous small vessels with a diameter of less than 3 mm and the hepatic parenchyma simultaneously. Subsequently, the ratio of the value in the intrahepatic venous small vessels was divided by the value in the hepatic parenchyma to generate the elastic ratio.

The elasticity of the hepatic vein was used as the reference because the elasticity of the veins does not change over time, since they do not undergo

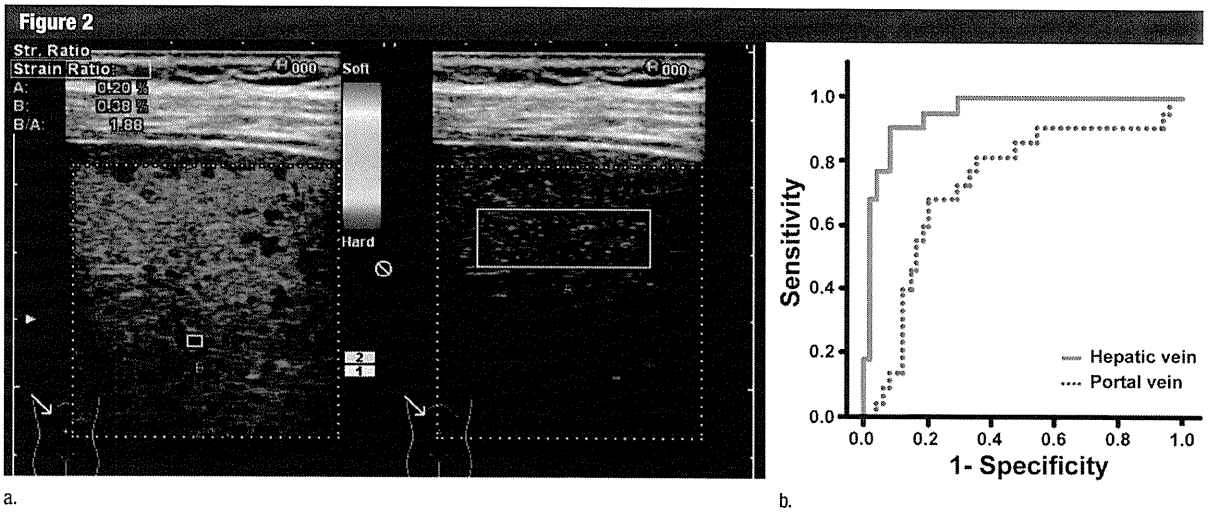

Figure 2: **(a)** The elastic ratio is measured between the tissue compressibility of the liver (right) and that of the intrahepatic small vessel (left). Red indicates that tissue is soft, and blue indicates that it is hard. Information about displacement becomes the basis of the elastic information and is obtained by using a supersonic wave signal. **(b)** Receiver operating characteristic (ROC) curves of the elastic ratio obtained by using the hepatic vein or portal vein as an internal control.

transformations with disease, such as arteriosclerosis, and it also does not increase or decrease even when liver parenchyma becomes stiffer. Thus, small vessels with a diameter of 3 mm in the liver were used as the standard for computing the elasticity ratio, and the ROI was set as large as possible (usually 0.3 × 0.5 cm). The ROI in the liver parenchyma was placed 1 cm from the liver surface and was 2 × 1 cm in size. A higher elastic ratio indicates harder hepatic elasticity, corresponding to a higher stage of fibrosis. None of the patients had liver tumors in the measurement site that might have interfered with the real-time tissue elastography.

Observers

Two hepatologists (M.H. and Y. Koizumi, with 13 and 6 years of experience, respectively) performed the liver stiffness evaluation with real-time tissue elastography; each had already performed at least 100 liver stiffness evaluations (M.H., 350; Y. Koizumi, 120) prior to the beginning of the study. Each observer measured the elastic ratio five times at four sites (Fig 1b). The second observer was blinded to the results of the first observer. Measurement time for each measurement site (time from the beginning of measurement until completion to identify the elastic ratio with five measurements after placing the ROI) was recorded for each observer. For measurement site IV, the measurement time included the time for movement of the patient.

Liver Histologic Assessment

US-guided percutaneous liver biopsy (1.6-mm-diameter and 150-mm-long needle, suction technique) was performed within 1 week after hospitalization. Liver biopsy samples less than 12 mm long were excluded, because a sampling error for identifying liver fibrosis may occur with such samples (4). Liver biopsy samples were fixed in formalin and embedded in paraffin. Slices (4 μm thick) were stained with hematoxylin-eosin and impregnated with silver. Liver biopsies that contained fewer than five portal tracts (except for cirrhosis) were excluded from the histologic analysis. Fibrosis was staged by two pathologists (one of whom was I.K., with 16 years of experience), who were blinded to all patient characteristics. Fibrosis was staged on a four-point scale according to METAVIR (F0 indicated no fibrosis; F1, portal fibrosis without septa; F2, portal fibrosis and few septa; F3, numerous septa without cirrhosis; F4, cirrhosis) (15). Activity was graded according to METAVIR as A0, none; A1, mild; A2, moderate; and A3, severe (16). Lipid share was defined as mild, 0%–30%; moderate, 30%–60%; and severe, more than 60%.

Serum Fibrosis Markers

Levels of the following blood parameters were determined: aspartate aminotransferase, alanine aminotransferase, total bilirubin, platelets, gamma-glutamyl transferase, cholesterol, urea, hyaluronic acid, type IV collagen, cholinesterase, α1 and α2 globulins, β globulins, γ-globulins, prothrombin index, apolipoprotein-A1, haptoglobin, and ferritin. The aspartate aminotransferase (AST)–to–platelet ratio index (17) was calculated as follows: (AST/UNL · 100)/platelet count. (UNL is the upper limit of the normal aspartate aminotransferase.) The FibroIndex (18) was calculated as 1.738 − 0.064 (platelet count) + 0.005 (AST) + 0.463 (gammaglobulin). Forns score (19) was calculated as 7.811 − 3.131 ln(platelet count) + 0.781 ln(gamma-glutamyl transferase) + 3.467 ln(age) − 0.014 (cholesterol). Hepascore (20) was calculated as $y/(1 + y)$, $y = \exp[-4.185818 - (0.0249 \cdot \text{age}) + 0.7464 \cdot \text{sex}] + (1.0039 \cdot \alpha2\text{-macroglobulin}) + (0.0302 \cdot \text{hyaluronic acid}) + (0.0691 \cdot \text{bilirubin}) - (0.0012 \cdot \text{gamma-glutamyl transferase})$.

Statistical Analysis

The AUC of the elastic ratio was then compared with that derived from standard laboratory tests published in the literature, including the aspartate aminotransferase–to–platelet ratio index, FibroIndex, Forns score, and Hepascore (17–20). The ROC curve was prepared by using a statistical software package (JMP, version 8; SAS Institute Japan, Tokyo, Japan).

The diagnostic performance of liver stiffness evaluation and fibrosis was determined in terms of sensitivity, specificity, positive predictive value, negative predictive value, diagnostic accuracy, and AUC. The optimal cutoff values for liver stiffness were chosen to maximize the sum of sensitivity and specificity, and positive and negative predictive values were computed for those cutoff values.

Stiffness measurements were not normally distributed. Therefore, the elastic ratio was compared with the categories of the consensus fibrosis stage by using the Kruskal-Wallis nonparametric analysis of variance test. Correlations between the elastic ratio and the histologic fibrosis stage were also analyzed by using Spearman correlation coefficients.

The correlations between the values of each observer's real-time tissue elastography measurements, as well as the site differences, were evaluated by calculating κ coefficients and ICCs. The κ coefficient was defined as follows: poor, $\kappa < 0.4$; fair to good, $0.4 \leq \kappa < 0.75$; and excellent, $0.75 \leq \kappa$ (21). The ICC was defined as follows: slight, $0 \leq ICC < 0.20$; fair, $0.21 \leq ICC < 0.40$; moderate, $0.41 \leq ICC < 0.60$; substantial, $0.61 \leq ICC < 0.80$; and almost perfect, $ICC > 0.81$ (22).

The estimated sample sizes according to the two-sample Student *t* test in the F1–F3 group and F4 groups were 20 and 20 respectively, given a type I error of .05, a type II error of .2, and an effect size of 1.785. Multivariate stepwise logistic regression models were used to identify independent significant factors among serum fibrosis markers, METAVIR fibrosis stage, and activity grade, steatosis, BMI, and skin fold thickness for the elastic ratio determined with real-time tissue elastography. The statistical analyses were performed by using the JMP statistical software.

Table 1

Patient Characteristics

Characteristic*	All Patients (*n* = 70)	Men (*n* = 46)	Women (*n* = 24)
Age (y)	65.5 ± 11.7	66.6 ± 10.3	63.4 ± 13.9
BMI (kg/m^2)	23.2 ± 3.37	22.8 ± 3.05	23.9 ± 3.82
ALT level (IU/L)	42.8 ± 31.4	46.3 ± 35.0	35.9 ± 21.9
Serum albumin level (g/dL)	3.68 ± 0.60	3.61 ± 0.61	3.81 ± 0.57
Platelet count (10^4/μL)	14.1 ± 7.12	14.1 ± 7.68	14.1 ± 6.05
Prothrombin time (%)	91.6 ± 18.1	89.3 ± 17.7	95.9 ± 18.4
Total bilirubin (mg/dL)	0.9 ± 0.44	0.95 ± 0.49	0.77 ± 0.30
GGT level (IU/L)	55.5 ± 46.8	62.6 ± 48.1	41.9 ± 41.6
Child-Pugh class			
A	63	40	23
B	7	6	1
C	0	0	0
Histologic fibrosis stage			
F1	12	6	6
F2	16	10	6
F3	19	12	7
F4	23	18	5
Histologic activity grade			
A0	1	1	0
A1	67	44	23
A2	2	1	1
A3	0	0	0
Histologic steatosis			
Mild	68	46	22
Moderate	2	0	2
Severe	0	0	0

Note.—Data are means ± standard deviations or numbers of patients.

* ALT = alanine aminotransferase, GGT = gamma-glutamyl transferase.

Results

Patients

Between January 2009 and September 2009, 70 patients met the inclusion criteria (Table 1). There were no significant differences in age ($P = .54$) or BMI ($P = .31$) between men and women. Gamma-glutamyl transferase was significantly higher in men ($P = .02$), but no significant difference was seen in the other biochemical tests between men and women (Table 1).

The rates of interobserver agreement in determining each fibrosis stage at each site were: site I, 81.4% (57 of 70 patients); site II, 71.4% (50 of 70 patients); site III, 74.3% (52 of 70 patients); and site IV, 75.7% (53 of 70 patients). For F4 or non-F4, the rate of interobserver agreement was: site I, 97.1% (68 of 70 patients); site II, 88.6% (62 of 70 patients); site III, 88.6% (62 of 70 patients); and site IV, 92.9% (65 of 70 patients). The mean κ value for F4 or non-F4 according to the elastic ratio was excellent at each site (site I, $\kappa = 0.94 \pm 0.04$ [standard error of the mean]; site II, $\kappa = 0.77 \pm 0.075$; site III, $\kappa = 0.77 \pm 0.08$; and site IV, $\kappa = 0.85 \pm 0.06$) (Table 2). At sites I–IV, the κ value, ICCs and 95% CIs indicated that the interobserver agreement was almost the same. The time for measurement was within 5 minutes for each measurement site, and the total measurement time for four sites was not significantly different between the two examiners ($P = .93$).

Table 2

Influence of Measurement Site on Interobserver Agreement

Parameter	Measurement Site				
	I	II	III	IV	All
ICC	0.95	0.92	0.91	0.94	0.97
95% CI	0.92, 0.97	0.87, 0.95	0.83, 0.93	0.90, 0.96	0.95, 0.98
Diagnosis of F1–F4 fibrosis (κ)	0.73	0.60	0.57	0.66	0.64
Diagnosis of F4 or non-F4 fibrosis (κ)	0.94	0.77	0.77	0.86	0.84
Measurement time for M.H. (min)	2.78 ± 1.38	2.92 ± 1.31	2.78 ± 1.38	3.12 ± 1.47	11.7 ± 1.66
Measurement time for Y. Koizumi (min)	2.82 ± 1.41	2.95 ± 1.29	2.77 ± 1.35	3.23 ± 1.41	11.9 ± 1.83

Figure 3

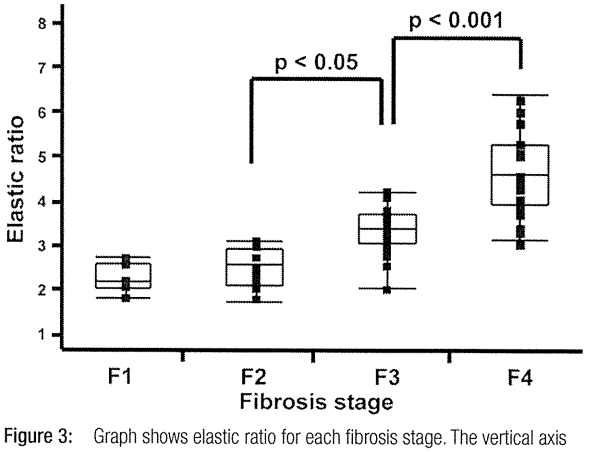

Figure 3: Graph shows elastic ratio for each fibrosis stage. The vertical axis is logarithmic scale. Tops and bottoms of the boxes = 1st and 3rd quartiles. The length of the box thus represents the interquartile range within which 50% of the values are located.

Figure 4

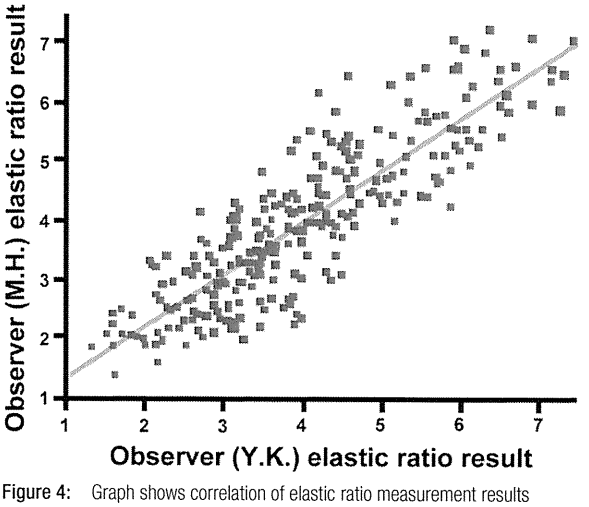

Figure 4: Graph shows correlation of elastic ratio measurement results between two examiners (Y. Koizumi and M.H., $r^2 = 0.869$, $P < .0001$).

Relationship between Liver Elastic Ratio and Histologic Parameters

The median value (95% CI) of the liver elastic ratio compared with the METAVIR fibrosis stage is shown in Figure 3: F1, 2.21 (1.94, 2.70); F2, 2.69 (2.29, 2.97); F3, 3.42 (3.07, 3.65); and F4, 4.66 (4.40, 4.93). The elastic ratios of each METAVIR fibrosis stage at liver biopsy differed significantly from each other (F2 vs F3, $r^2 = 0.36$, $P = .02$; F3 vs F4, $r^2 = 0.41$, $P < .001$). We found a significant correlation between fibrosis stage and the elastic ratio ($\rho = 0.82$, $P < .001$). However, there was no correlation between the METAVIR activity grade and the elastic ratio ($P = .36$). The elastic ratios identified by the two examiners were strongly correlated (Fig 4) and did not differ significantly. The optimal elastic ratio cutoff values obtained for the entire population, as well as the corresponding sensitivities and specificities, are shown in Table 3. The apparent cutoff values for F ≥ 2 (2.79) and F ≥ 3 (3.25) were close, but F ≥ 3 had higher sensitivity and specificity (85.4% and 96.4%) than F ≥ 2 (82.8% and 90.9%); however, the differences were not significant (sensitivity, $P = .67$; specificity, $P = .10$). A clear cutoff value (3.93) was obtained for F = 4, with sensitivity and specificity of 90.9% and 91.5%, respectively.

Mean real-time tissue elastography liver parenchyma values were as follows: site I, 0.07 ± 0.05 (standard deviation); site II, 0.08 ± 0.045; site III, 0.08 ± 0.06; site IV, 0.09 ± 0.05; and total, 0.08 ± 0.05 ($P = .09$). The mean absolute value of the hepatic vein vessels on real-time tissue elastography did not differ significantly according to site (site I, 0.25 ± 0.14; site II, 0.25 ± 0.12; site III, 0.26 ± 0.19; site IV, 0.25 ± 0.12; and total, 0.25 ± 0.13, $P = .94$).

Relationship between Liver Elastic Ratio and Fibrosis Blood Tests

The AUCs for diagnosis of fibrosis with elastic ratio, hyaluronic acid, type IV collagen (Fig 5a), aspartate aminotransferase-to-platelet ratio index, FibroIndex, Forns score, and Hepascore (Fig 5b) were 0.95, 0.32, 0.73, 0.76, 0.76, 0.87, and 0.70, respectively (Table 4). In the multivariate stepwise regression analysis, METAVIR fibrosis stage ($P < .0001$) and prothrombin time ($P = .0013$) were

Table 3

Elastic Ratio for Determination of METAVIR F Stage

Parameter	F ≥ 2 (F1 vs F2–F4)	F ≥ 3 (F1–F2 vs F3–F4)	F = 4 (F1–F3 vs F4)
AUC	0.89	0.94	0.95
Optimal cutoff	2.73	3.25	3.93
Sensitivity (%)	82.8	85.4	90.9
Specificity (%)	90.9	96.4	91.5
Positive predictive value (%)	98.0	97.2	83.3
Negative predictive value (%)	50.0	81.8	95.6

Table 4

Results of Comparison between Real-time Elastography and Fibrosis Blood Tests

Parameter	Real-Time Elastography	APRI*	Forns Score	FibroIndex	Hepascore
AUC	0.95	0.76	0.87	0.76	0.70
Sensitivity (%)	90.9	81.8	68.2	63.6	63.4
Specificity (%)	91.5	74.4	95.8	87.5	70.8

* APRI = aspartate aminotransferase–to–platelet ratio index.

Figure 5

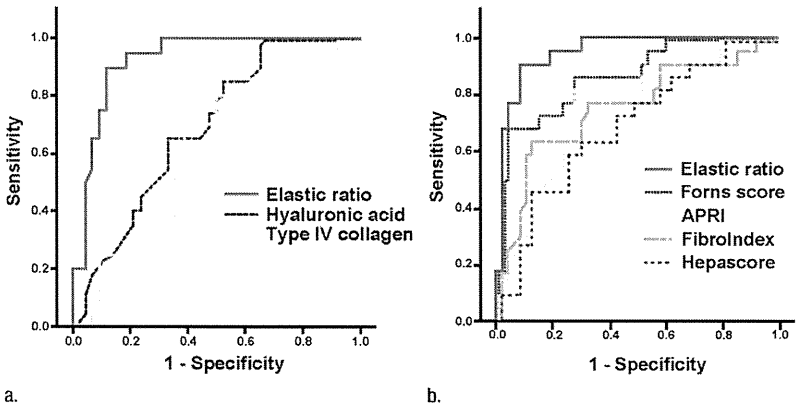

Figure 5: **(a, b)** ROC curves for diagnosis of liver fibrosis (F4) with real-time elastography. The AUC for the diagnosis of clinically important liver fibrosis or cirrhosis (F4) by using the EUB-7500 (Hitachi Medical Systems) device is superior to the results with **(a)** blood parameters or **(b)** calculated fibrosis indexes. *APRI* = aspartate aminotransferase–to–platelet ratio index.

independently associated with the elastic ratio.

Skin Fold Thickness and BMI

Interobserver agreement for elastic ratio was excellent when the skin fold thickness was less than 20 mm and BMI was less than 25 kg/m^2. However, for patients with a skin fold thickness greater than 20 mm or a BMI greater than 25 kg/m^2, the interobserver agreement was not as good (Table 5).

Discussion

There are many reports and approaches to evaluating liver stiffness without liver biopsy. Among them, the FibroScan appears useful (23,24), but there are few reports about its reproducibility. Boursier et al (10) reported that the reproducibility of the liver hardness measurement obtained by using the FibroScan differs according to measurement position. Since the absolute value of liver stiffness at real-time tissue elastography was variable, we established a procedure to obtain reproducibility by using the signal of the small hepatic veins as a reference. Using the elastic ratio, we found no difference in reproducibility for four measurement positions. Moreover, real-time tissue elastography has other advantages compared with the FibroScan or the acoustic radiation force impulse (Appendix E1 [online]).

We checked the reproducibility of the elastic ratio derived from real-time tissue elastography. The real-time tissue elastography procedure reported previously (13) involves applying pressure in the intercostal space with a probe; thus, when the pressure applied with the probe differs, the real-time tissue elastography value changes. This means that the value of liver stiffness differs not only with each observer, but also within the same observer. Therefore, we put a probe in the intercostal space and conducted the examination with no added pressure, because when observers add pressure during measurement, observer bias may occur. The liver itself receives pressure from the heartbeat automatically, so the elastic ratio could be measured without adding any pressure with the probe. Thus, observer variability can be lessened with this procedure.

Fatty change of the liver affects the evaluation of liver stiffness with the FibroScan (11). We performed a multivariate stepwise regression analysis to identify factors that affect real-time tissue elastography. Skin fold thickness, BMI, and liver steatosis were not identified as factors affecting the elastic ratio determined by using real-time tissue elastography, while fibrosis stage was a factor. Therefore, real-time tissue elastography may measure the degree of fibrosis. Only for patients with a skin fold thickness greater than 20 mm or BMI greater than 25 kg/m^2 did the interobserver agreement have a wider range, though the difference was not significant (perhaps owing to the small

Table 5

Results according to BMI and Skin Fold Thickness

Parameter	Group 1	Group 2	Group 3	Group 4	Group 5
BMI (kg/m^2)	<19 (n = 5)	≥19 To <22 (n = 21)	≥22 To <25 (n = 27)	≥25 To <28 (n = 9)	≥28 (n = 8)
ICC	0.91	0.94	0.90	0.88	0.88
95% CI	−0.39, 1.0	0.81, 0.98	0.77, 0.96	0.36, 0.94	0.39, 0.98
Skin fold thickness (mm)	<15 (n = 15)	≥15 To <20 (n = 37)	≥20 To <25 (n = 13)	≥25 (n = 5)	...
ICC	0.95	0.92	0.83	0.81	...
95% CI	0.83, 0.98	0.84, 0.96	0.51, 0.95	−0.68, 1.00	...

sample size). The elastic ratio could be calculated for the two patients with BMIs greater than 30 kg/m^2. Further studies involving more severely obese individuals will be needed to confirm the usefulness of real-time tissue elastography for such patients.

The elastic ratio obtained by using real-time tissue elastography performed better than serum fibrosis markers and scores of fibrotic change based on blood laboratory tests. However, our study still had limitations. It is difficult to evaluate certain types of patients with B mode US, including those with thick, fat tissue under the skin; a history of abdominal operations; difficulty stopping breathing; too much liver atrophy; or a large amount of ascites. We had only two observers, each with experience with the modality, and used only one US machine. Therefore, our results might not be applicable to other individuals with less experience. Our cutoffs for determination of accuracy were based on our own results and therefore are likely overestimates of performance.

In summary, in patients with chronic hepatitis C, real-time tissue elastography allows for noninvasive assessment of fibrosis that does not vary with the sites we tested or by observer and performs better than fibrosis indexes calculated by using blood laboratory tests.

Acknowledgments: The authors thank Ravi Managuli, PhD, RDMS (Department of Bioengineering, University of Washington, Seattle, Wash), for assistance in editing the technical comments and Yoshiko Soga, MD, PhD (Pathology Division, Ehime University Hospital, Ehime, Japan), for evaluating the histologic features of liver specimens.

References

1. Lauer GM, Walker BD. Hepatitis C virus infection. N Engl J Med 2001;345(1):41–52.
2. Strader DB, Wright T, Thomas DL, Seeff LB; American Association for the Study of Liver Diseases. Diagnosis, management, and treatment of hepatitis C. Hepatology 2004; 39(4):1147–1171. [Published correction appears in Hepatology 2004;40(1):269.]
3. Cadranel JF, Rufat P, Degos F. Practices of liver biopsy in France: results of a prospective nationwide survey. For the Group of Epidemiology of the French Association for the Study of the Liver (AFEF). Hepatology 2000;32(3):477–481.
4. Pagliaro L, Rinaldi F, Craxì A, et al. Percutaneous blind biopsy versus laparoscopy with guided biopsy in diagnosis of cirrhosis: a prospective, randomized trial. Dig Dis Sci 1983;28(1):39–43.
5. Regev A, Berho M, Jeffers LJ, et al. Sampling error and intraobserver variation in liver biopsy in patients with chronic HCV infection. Am J Gastroenterol 2002;97(10):2614–2618.
6. Rousselet MC, Michalak S, Dupré F, et al. Sources of variability in histological scoring of chronic viral hepatitis. Hepatology 2005;41(2):257–264.
7. Sandrin L, Fourquet B, Hasquenoph JM, et al. Transient elastography: a new noninvasive method for assessment of hepatic fibrosis. Ultrasound Med Biol 2003;29(12): 1705–1713.
8. Friedrich-Rust M, Ong MF, Martens S, et al. Performance of transient elastography for the staging of liver fibrosis: a meta-analysis. Gastroenterology 2008;134(4):960–974.
9. Friedrich-Rust M, Wunder K, Kriener S, et al. Liver fibrosis in viral hepatitis: noninvasive assessment with acoustic radiation force impulse imaging versus transient elastography. Radiology 2009;252(2):595–604.
10. Boursier J, Konaté A, Gorea G, et al. Reproducibility of liver stiffness measurement by ultrasonographic elastometry. Clin Gastroenterol Hepatol 2008;6(11):1263–1269.
11. Fraquelli M, Rigamonti C, Casazza G, et al. Reproducibility of transient elastography in the evaluation of liver fibrosis in patients with chronic liver disease. Gut 2007;56(7): 968–973.
12. Yamakawa M, Nitta N, Shiina T, et al. High-speed freehand tissue elasticity imaging for breast diagnosis. Jpn J Appl Phys 2003;42: 3265–3270.
13. Friedrich-Rust M, Ong MF, Herrmann E, et al. Real-time elastography for noninvasive assessment of liver fibrosis in chronic viral hepatitis. AJR Am J Roentgenol 2007; 188(3):758–764.
14. Shiina T. Real time tissue elasticity imaging using the combined autocorrelation method. J Med Ultrason 1999;26(2):57–66.
15. Intraobserver and interobserver variations in liver biopsy interpretation in patients with chronic hepatitis C. The French METAVIR Cooperative Study Group. Hepatology 1994; 20(1 pt 1):15–20.
16. Bedossa P, Poynard T. An algorithm for the grading of activity in chronic hepatitis C. The METAVIR Cooperative Study Group. Hepatology 1996;24(2):289–293.
17. Wai CT, Greenson JK, Fontana RJ, et al. A simple noninvasive index can predict both significant fibrosis and cirrhosis in patients with chronic hepatitis C. Hepatology 2003;38(2):518–526.
18. Koda M, Matunaga Y, Kawakami M, Kishimoto Y, Suou T, Murawaki Y. FibroIndex, a practical index for predicting significant fibrosis in patients with chronic hepatitis C. Hepatology 2007;45(2):297–306.
19. Forns X, Ampurdanès S, Llovet JM, et al. Identification of chronic hepatitis C patients without hepatic fibrosis by a simple predictive model. Hepatology 2002;36(4 pt 1): 986–992.
20. Adams LA, Bulsara M, Rossi E, et al. Hepascore: an accurate validated predictor of liver fibrosis in chronic hepatitis C infection. Clin Chem 2005;51(10):1867–1873.
21. Fleiss JL. Statistical methods for rates and proportions. 2nd ed. New York, NY: Wiley, 1981;218.
22. Landis JR, Koch GG. The measurement of observer agreement for categorical data. Biometrics 1977;33(1):159–174.
23. Harada N, Soejima Y, Taketomi A, et al. Assessment of graft fibrosis by transient elastography in patients with recurrent hepatitis C after living donor liver transplantation. Transplantation 2008;85(1):69–74.
24. Fraquelli M, Rigamonti C. Diagnosis of cirrhosis by transient elastography: what is hidden behind misleading results. Hepatology 2007;46(1):282; author reply 282–283.

Hepatic Elasticity in Patients With Ascites: Evaluation With Real-Time Tissue Elastography

Masashi Hirooka[1]
Yohei Koizumi
Yoichi Hiasa
Masanori Abe
Yoshio Ikeda
Bunzo Matsuura
Morikazu Onji

OBJECTIVE. Transient elastography is a rapid, noninvasive, and reproducible approach to assessment of liver fibrosis by measurement of liver elasticity. However, transient elastographic measurements are of limited utility in patients with ascites or severe obesity. The aim of this study was to determine whether measurements of liver stiffness with real-time tissue elastography can be altered for patients with ascites.

SUBJECTS AND METHODS. The subjects were 54 patients being treated at a university hospital between January and December 2009. In 42 patients, real-time tissue elastography to evaluate liver stiffness was performed before and after injection to produce artificial ascites for radiofrequency ablation. The other 12 patients had ascites due to cirrhosis, and liver stiffness was measured with real-time tissue elastography before and after control of ascites.

RESULTS. Elastic ratios evaluated with real-time tissue elastography did not differ significantly before and after injection for artificial ascites or before and after control of ascites. This ratio was the same for patients with and those without cirrhosis and was unaffected by distance between the body surface and the targeted liver area. Stable values thus were measured with real-time tissue elastography.

CONCLUSION. Liver stiffness can be measured reproducibly with real-time tissue elastography even in patients with ascites. This method has the potential of being superior to transient elastography for assessment of liver stiffness, particularly in patients with decompensated cirrhosis.

Keywords: ascites, elastic ratio, liver stiffness, real-time tissue elastography, reproducibility

DOI:10.2214/AJR.10.4867

Received April 21, 2010; accepted after revision October 11, 2010.

Supported in part by a grant-in-aid for scientific research (JSPS KAKENHI 21590848) to Y. Hiasa from the Japanese Ministry of Education, Culture, Sports, Science and Technology.

[1]All authors: Department of Gastroenterology and Metabology, Ehime University Graduate School of Medicine, Shitsukawa, Toon, Ehime 791-0295, Japan. Address correspondence to Y. Hiasa (hiasa@m.ehime-u.ac.jp).

WEB
This is a Web exclusive article.

AJR 2011; 196:W766–W771

0361–803X/11/1966–W766

© American Roentgen Ray Society

Liver biopsy is considered the reference standard for evaluation of hepatic fibrosis. However, this procedure is invasive and carries risk of life-threatening complications [1]. In addition, the reproducibility of liver biopsy in the assessment of fibrosis is limited because of sampling error and interobserver variability [2–6]. Transient elastography is a rapid, noninvasive, and reproducible approach to the assessment of liver fibrosis through the measurement of liver elasticity [7, 8]. Liver stiffness measured with transient elastography is associated strongly with the degree of liver fibrosis in patients with chronic hepatitis [9–12]. Although the accumulation of fibrillar extracellular matrix is certainly a major determinant of liver tissue stiffness during transient elastography, other factors associated with chronic liver disease, such as inflammatory infiltration, tissue necrosis, and edema, may affect the evaluation [13, 14]. Moreover, transient elastographic measurement is known to be limited in patients with severe obesity or ascites [15], and previous studies of transient elastography have excluded patients with ascites [3–6]. Ascites is a physical limitation to push-pulse technique because elastic waves do not propagate through liquids.

Investigations of transient elastography and real-time tissue elastography have proved the utility of noninvasive assessment of liver tissue stiffness in patients with chronic liver disease, such as viral hepatitis and cirrhosis [16]. Real-time tissue elastography is performed with B-mode sonography, and the method by which elasticity is measured with real-time tissue elastography differs from the method of transient elastography. Real-time tissue elastography has more potential for precise evaluation of liver stiffness than does transient elastography because, first, numerous pulses are transmitted and mean values of the frames are used and, second, elasticity can be measured with slight compression or

TABLE 1: Clinical Characteristics

Characteristic	Total (n = 54)	Artificial Ascites Group (n = 42)	Ascites Group (n = 12)
Male to female ratio	41/13	33/9	8/4
Age (y)	66.3 ± 8.0	66.0 ± 8.7	67.3 ± 4.8
Serologic findings			
Hepatic B surface antigen positive	10	7	3
Hepatitis C virus antibody positive	32	27	5
Negative both for HBs-antigen and hepatitis C virus antibody	12	8	4
Pathologic finding			
Hepatocellular carcinoma	49	37	12
Metastatic liver tumor	5	5	0
Child-Pugh class			
A	40	40	0
B	2	2	0
C	12	0	12
Metavir score[a]			
F0		5	
F1		0	
F2		3	
F3		5	
F4		29	

Note—Except for age, values are number of patients.
[a]The ascites group did not undergo biopsy.

relaxation of the body and echo signals are captured in real time. Furthermore, real-time tissue elastography can display tissue elasticity images and conventional B-mode images simultaneously. With this simultaneous display, anatomic correlations between elasticity images and B-mode images can be more readily understood than in transient elastography. The aim of the current study was to determine whether real-time tissue elastography is sufficiently precise for evaluation of liver stiffness in patients with ascites.

Subjects and Methods

Patients

The ethics committee of our institution approved all study protocols. Written informed consent to participate in the study was obtained before enrollment, in accordance with the principles of the Declaration of Helsinki. The subjects were 54 patients (41 men, 13 women; mean age, 66.3 ± 8.0 years; range, 47–81 years) treated at our institution between January and December 2009. The clinical backgrounds of the subjects are shown in Table 1. The study protocol is shown in Figure 1. Of the 54 patients, 42 patients had no ascites originally and were undergoing radiofrequency ablation of hepatocellular carcinoma and artificial ascites was being introduced in the procedure, as reported previously [16, 17]. Liver biopsy and real-time tissue elastography were performed before the artificial ascites injection. Real-time tissue elastography was repeated after induction of artificial ascites, and radiofrequency ablation was performed to manage the hepatocellular carcinoma nodule. Measurement of liver stiffness with real-time tissue elastography also was undertaken for the 12 patients who had ascites due to cirrhosis. All 12 patients had chronic liver disease diagnosed according to standard criteria with laboratory tests, sonography, CT, and endoscopy. Three patients had positive results for hepatitis B surface antigen; five had positive results for hepatitis C virus; and four had a history of alcohol abuse. Control of ascites was achieved in all 12 patients by sodium restriction and standard management of cirrhosis (diuretics with or without administration of IV albumin). Sonography was performed to confirm a decrease in ascites after these treatments. After ascites was controlled, real-time tissue elastography was repeated.

Exclusion criteria for enrollment in this study were body mass index of 25 or greater, platelet count less than 30,000/μL, use of hepatotoxic drugs in the 6 months before enrollment, vascular diseases of the liver, biliary tract disorders, cardiac failure, and pregnancy. All patients underwent laboratory tests at enrollment, including serum bilirubin, albumin, ammonia, aspartate aminotransferase, alanine aminotransferase, alkaline phosphatase, γ-glutamyl transpeptidase, platelet count, and creatinine and glucose concentrations.

Measurement of Hepatic Elasticity With Real-Time Tissue Elastography

Hepatic elasticity was measured with a real-time tissue elastographic system (EUB-7500, Hitachi Medical Systems) [18]. A linear probe (central frequency, 5.5 MHz; EUP-L52, Hitachi Medical Systems) was used. During real-time tissue elastography, B mode was used first for visualization of the liver and then elastographic mode was instituted. During elastography, areas of normal liver parenchyma appear green, and areas of increased liver stiffness appear blue (Fig. 2). Small intrahepatic vessels appear red. To reduce variation between individuals, we proposed use of the red signal as an internal control for evaluating stiffness of the liver parenchyma. We therefore first evaluated variability in the red signal in portal vessels and hepatic veins and then defined the red signal of hepatic veins as an internal control because these vessels had less variation than portal vessels.

Regions of interest were placed on small intrahepatic veins and the hepatic parenchyma at the same time, and each signal was evaluated. From those data, we calculated the ratio of the value of small

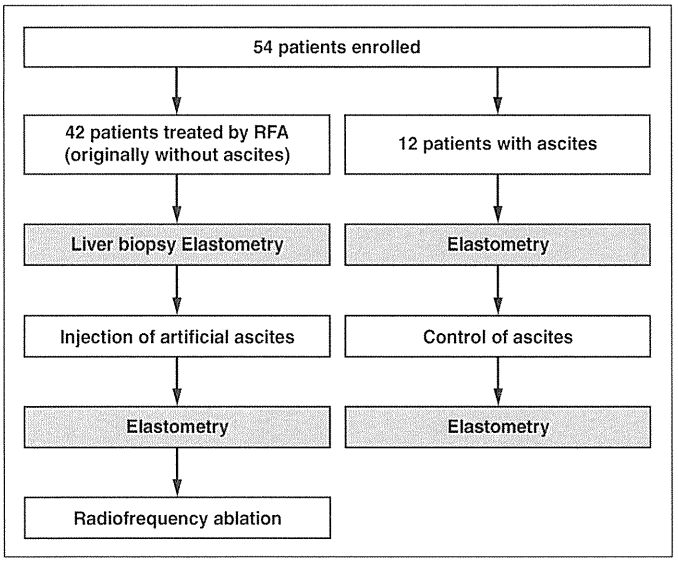

Fig. 1—Chart shows flow of participants through trial. For 42 of 54 patients, liver stiffness was measured before and after injection for artificial ascites for radiofrequency ablation (RFA). For 12 patients, who already had ascites at enrollment, real-time tissue elastography for evaluation of liver stiffness was performed before and after control of ascites.

intrahepatic veins to the value of hepatic parenchyma as the elastic ratio, a higher elastic ratio indicating greater hepatic elasticity. The region of interest placed in the liver parenchyma measured 2 × 1 cm. At the time of measurement, we placed a probe in the intercostal space. Bare minimum pressure was placed on the probe to ensure measurement universality. Because each heartbeat distorts the liver, the pressure on the liver needed for evaluation of liver stiffness with real-time tissue elastography was automatically produced by the heart. Observations were made by freehand technique, the probe being kept in position by application of slight manual pressure.

Liver Histologic Assessment

Ultrasound-guided percutaneous liver biopsy (suction technique with a needle 1.6 mm in diameter and 150 mm long) was performed before injection for artificial ascites. We excluded liver specimens shorter than 12 mm. Liver biopsy samples were fixed in formalin and embedded in paraffin. Sections 4 μm thick were stained with H and E and silver impregnation. Liver biopsy samples that contained fewer than five portal tracks (except for cirrhosis) were excluded from histologic analysis. Fibrosis was staged by two pathologists blinded to patient characteristics. The lesions were scored with the 4-point Metavir system (F0, no fibrosis; F1, portal fibrosis without septa; F2, portal fibrosis and few septa; F3, numerous septa without cirrhosis; F4, cirrhosis) [19]. Hepatitis activity was graded A0, none; A1, mild; A2, moderate; and A3, severe [20].

Injection of Ascites

All patients received premedication with an intramuscular injection of 25 mg of hydroxyzine and 15 mg of pentazocine while conscious. During each procedure, oxygen saturation and other vital signs were assessed regularly. A 14-gauge needle (Daimon Needle, Silux) with a metallic flat-cut trocar and a diamond-cut inner stylet was used for artificial ascites infusion under real-time sonographic guidance. The needle was inserted along the edge of the liver to avoid injury to the liver and adjacent organs. When the needle reached the abdominal cavity, the inner stylet was removed and 5% glucose solution was infused rapidly [16, 17]. After the area of ascites was discerned with B-mode ultrasound, liver stiffness was measured with real-time tissue elastography (Fig. 2).

Statistical Analysis

Quantitative variables are reported as mean ± SD. Differences of all variables in Tables 2 and 3 (i.e., distances from body surface to liver surface and elastic ratios) between the two groups (Fig. 3) were evaluated with the paired Student *t* test after confirmation of a normal distribution. The diagnostic performance of liver stiffness evaluation and fibrosis area was determined in terms of sensitivity, specificity, positive predictive value, negative predictive value, diagnostic reproducibility, and area under the receiver operating characteristic curve. Statistical analyses were performed with JMP software (version 8, SAS Institute Japan).

Results

The characteristics of the 42 patients (33 men, nine women; mean age, 66.0 ± 8.7 years) who underwent artificial ascites injection are shown in Table 1. The stage of liver fibrosis was F0 in five patients, F2 in three patients, F3 in five patients, and F4 in 29 patients. Forty patients had Child-Pugh class A disease, and two patients with cirrhosis had Child-Pugh class B disease. Seven patients had positive results for hepatitis B surface antigen and 27 for hepatitis C virus, and eight patients had negative results for both hepatitis B surface antigen and hepatitis C virus. Hepatocellular carcinoma nodules were identified in 37 patients, and the other five patients had metastatic liver tumors. Two nodules were located in segment IV, 23 in segment VI, two in segment VII, and 15 in segment VIII. The total volume of injected artificial ascites fluid was 1097.1 ± 199.2 mL (range, 780–1500 mL). The mean distance between the body surface and the surface of the liver was 22.5 ± 3.3 mm (range, 16.5–31.1 mm).

Among the patients who underwent artificial ascites injection, the mean elastic ratio was 3.78 ± 0.87 before injection and 3.75 ± 0.76 after injection ($p = 0.973$), not a significant

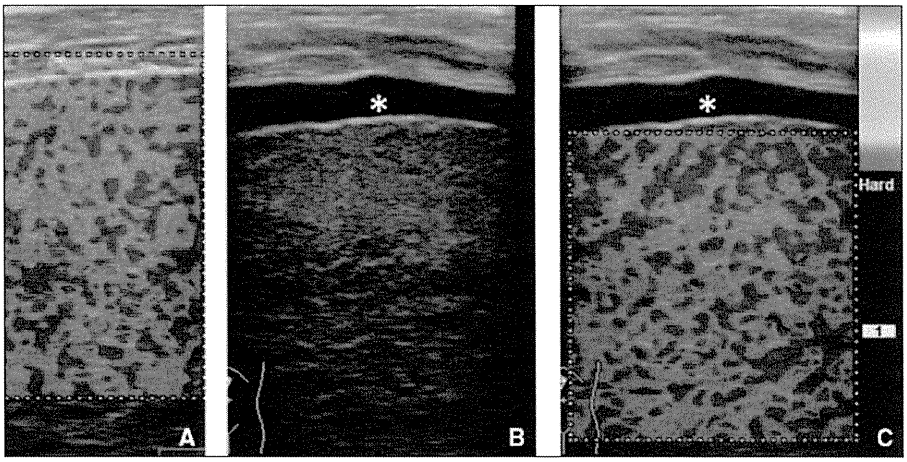

Fig. 2—54-year-old man undergoing radiofrequency ablation of hepatocellular carcinoma.
A, Tissue elastographic image before injection for artificial ascites shows elastic ratio of 2.79.
B, B-mode ultrasound image shows layer of artificial ascites (*asterisk*).
C, Tissue elastographic image shows elastic ratio of 2.80 in presence of ascites (*asterisk*).

TABLE 2: Liver Stiffness Before and After Artificial Ascites Injection

Characteristic	*n*	Before	After	Paired Difference	*p*
Distance (mm)[a]		10.51 ± 1.48	22.61 ± 3.35	12.100	< 0.0001
Elastic ratio	42	3.78 ± 0.87	3.75 ± 0.76	−0.0293	0.973
Cirrhosis[b]	29	4.22 ± 0.40	4.26 ± 0.39	−0.0355	0.980
No cirrhosis[c]	13	2.69 ± 0.62	2.70 ± 0.66	−0.0154	0.680
Elastic ratios substratified by volume of artificial ascites (mL)					
< 1000	28	3.92 ± 0.73	3.95 ± 0.75	−0.0332	0.957
≥ 1000	14	3.39 ± 0.99	3.42 ± 1.03	−0.0214	0.790

[a]Between body surface and surface of liver.
[b]Metavir F4.
[c]Metavir scores other than 4.

TABLE 3: Liver Stiffness Before and After Control of Ascites

Parameter	Before	After	Paired Difference	*p*
Distance (mm)[a]	28.48 ± 2.82	18.13 ± 2.52	18.133	< 0.0001
Elastic ratio	5.46 ± 0.52	5.51 ± 0.45	0.0533	0.766

[a]From body surface to surface of liver.

change (Fig. 3A). Moreover, the amount of ascites and the distance between the abdominal skin and the liver surface had no influence on elastic ratio (Table 2). Areas under the receiver operating characteristic curves of elastic ratios for predicting F0, greater than F2, and F4 were 1.00 ($p < 0.0001$), 0.95 ($p < 0.0001$), and 0.92 ($p < 0.0001$).

All 12 patients (eight men, four women; mean age, 67.3 ± 4.8 years) who already had ascites due to cirrhosis (Table 1) had Child-Pugh class C disease. The mean distance between the body surface and the surface of the liver was 28.4 ± 2.8 mm (range, 21.9–32.0 mm) before ascites control and was significantly lower after control. The elastic ratio was measured in all 12 patients (Table 3) and was not significantly changed after control of ascites (Table 3 and Fig. 3B). The mean interval between elastographic measurements before and after ascites control was 20.3 ± 5.8 days.

Discussion

This study confirmed that liver stiffness can be evaluated in a stable manner with real-time tissue elastography and B-mode sonography even in patients with ascites. The reference standard for assessing liver fibrosis is liver biopsy, but that technique is invasive, and many patients subsequently report pain [21]. The procedure also carries a risk of severe complications, at a rate of 3.1 cases per 1000 patients [22]. Sampling error also can complicate evaluation of liver stiffness because the biopsy specimen represents 1/50,000 of the total liver [1]. Moreover, interobserver and intraobserver discrepancies of 10–20% in assessing hepatic fibrosis have been reported [6, 23, 24], potentially contributing to the misdiagnosis of cirrhosis.

In contrast to liver biopsy, transient elastography with ultrasound is painless and carries little risk of complications. Liver stiffness is measured in a cylindric volume approximately 1 cm in diameter by 2 cm long, representing a volume 100 times larger than a biopsy specimen. Transient elastography also is more representative of the entire hepatic parenchyma [21] and is well accepted. Transient elastography does, however, have limitations in the measurement of liver stiffness. Elastometry by transient elastography cannot be used in patients with ascites, even if clinically undetected. Ascites poses a physical impediment to push-pulse technique because elastic waves do not propagate through liquids. Accurate elastic measurements thus cannot be obtained by transient elastography in patients with advanced cirrhosis because most patients with cirrhosis have ascites. In contrast, elastometry with real-time tissue elastography can be performed on patients with ascites, for the following reasons.

First, real-time tissue elastography is a combined autocorrelation method that entails color Doppler imaging [25], whereas transient elastography entails the Doppler method. In the Doppler method, which has only two signals, many pulses are transmitted, and the mean values of the frames are used. In real-

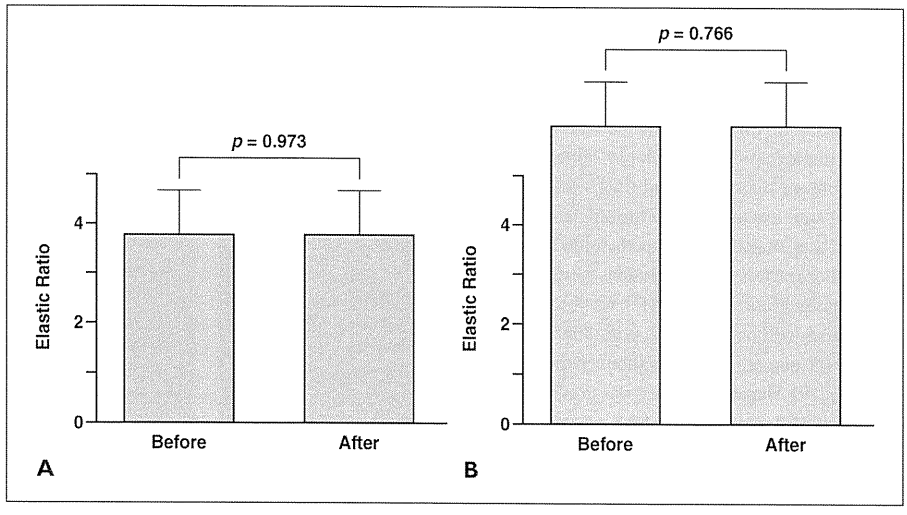

Fig. 3—Elastic ratios. No significant differences were found between real-time tissue elastographic measurements with and without ascites; *p* is based on paired Student *t* test of paired differences of ratios.
A, Graph shows results before and after artificial ascites injection.
B, Graph shows results before and after successful control of ascites.

time tissue elastography, strain images are acquired and combined autocorrelation of echo signals generated before and after each compression (central frequency, 5.5 MHz; scanning rate, 360 lines/frame). Real-time tissue elastography is performed in B mode, whereas transient elastography is performed in A mode. As a result, real-time tissue elastography can be used to measure liver stiffness even in patients with ascites.

Second, for real-time tissue elastography, the compression needed for sonographic measurement is provided physiologically by spontaneous respiratory motion and vascular and cardiac pulsations. Thus only bare minimum compression with the linear probe is necessary for real-time tissue elastography, compared with the push pulse from the body surface required for transient elastography. In patients with ascites, the push pulse is prevented from reaching the liver parenchyma by the ascites. Real-time tissue elastography thus has more potential for precise evaluation of liver stiffness than does transient elastography.

We performed this prospective study with the participation of patients who were about to undergo radiofrequency ablation facilitated by artificial ascites. The results showed no significant difference in elastic ratios before and after injection for artificial ascites (Table 2). The differences in the noncirrhosis ($p = 0.680$) and cirrhosis ($p = 0.980$) groups were attributed to the heterogeneity of Metavir stage in the group without cirrhosis (all Metavir scores other than F4) compared with the cirrhosis group (Metavir score F4). The artificial ascites injected consisted of 5% glucose, differing from natural ascites fluid, which contains albumin, globulins, and electrolytes. To study differences between artificial ascites and natural ascites, we also performed real-time tissue elastography before and after treatments to control ascites in patients with cirrhosis who had natural ascites. The results showed that natural ascites, like artificial ascites, did not influence real-time tissue elastographic measurement (Table 3). Another problem for measurement with real-time tissue elastography is that liver stiffness can be measured within a depth of 5 cm. Because of the thickness of subcutaneous fat, however, the distance between the body surface and the liver has to be approximately 3 cm for precise measurement with this technique. If a patient has extreme ascites, real-time tissue elastography should be performed after ascites is controlled, shortening the distance between the body surface and the liver surface to within 3 cm. In such cases, stiffness of the left hepatic lobe can be evaluated, because less ascites is usually seen between the left lobe and the surface than between the right lobe and the surface. Otherwise, real-time tissue elastography with an endoscopic ultrasound probe can be considered [26, 27].

This study had limitations. Most of the patients enrolled had Metavir stage F4 disease, and no patient had F1 disease. The distribution of the patient sample was inappropriate for accurate assessment of fibrosis. The maximal distance between the body surface and the liver surface was 32.0 mm for real-time tissue elastography. For patients with a distance of 32.0 mm or more due to ascites or fat, a region of interest cannot be placed in the liver. This represents a mechanical limitation of real-time tissue elastography, and improvements in the hardware are required to address the issue.

Conclusion

Liver stiffness can be measured reproducibly with real-time tissue elastography even in patients with ascites. Because transient elastography cannot be used to evaluate liver stiffness in patients with cirrhosis and ascites, the real-time tissue elastographic method may have better potential than transient elastography for identification of liver stiffness. Moreover, real-time tissue elastography is noninvasive and is associated with less sampling error than liver biopsy and thus has advantages for both clinicians and patients when data on liver stiffness are needed to determine suitable treatment and evaluate prognosis.

References

1. Bravo AA, Sheth SG, Chopra S. Liver biopsy. *N Engl J Med* 2001; 344:495–500
2. Abdi W, Millan JC, Mezey E. Sampling variability on percutaneous liver biopsy. *Arch Intern Med* 1979; 139:667–669
3. Bedossa P, Dargere D, Paradis V. Sampling variability of liver fibrosis in chronic hepatitis C. *Hepatology* 2003; 38:1449–1457
4. Cadranel JF, Rufat P, Degos F. Practices of liver biopsy in France: results of a prospective nationwide survey. Group of Epidemiology of the French Association for the Study of the Liver (AFEF). *Hepatology* 2000; 32:477–481
5. Maharaj B, Maharaj RJ, Leary WP, et al. Sampling variability and its influence on the diagnostic yield of percutaneous needle biopsy of the liver. *Lancet* 1986; 1:523–525
6. Regev A, Berho M, Jeffers LJ, et al. Sampling error and intraobserver variation in liver biopsy in patients with chronic HCV infection. *Am J Gastroenterol* 2002; 97:2614–2618
7. Sandrin L, Tanter M, Gennisson JL, Catheline S, Fink M. Shear elasticity probe for soft tissues with 1-D transient elastography. *IEEE Trans Ultrason Ferroelectr Freq Control* 2002; 49:436–446
8. Sandrin L, Fourquet B, Hasquenoph JM, et al. Transient elastography: a new noninvasive method for assessment of hepatic fibrosis. *Ultrasound Med Biol* 2003; 29:1705–1713
9. Ziol M, Handra-Luca A, Kettaneh A, et al. Noninvasive assessment of liver fibrosis by measurement of stiffness in patients with chronic hepatitis C. *Hepatology* 2005; 41:48–54
10. Castera L, Vergniol J, Foucher J, et al. Prospective comparison of transient elastography, Fibrotest, APRI, and liver biopsy for the assessment of fibrosis in chronic hepatitis C. *Gastroenterology* 2005; 128:343–350
11. Ganne-Carrie N, Ziol M, de Ledinghen V, et al. Accuracy of liver stiffness measurement for the diagnosis of cirrhosis in patients with chronic liver diseases. *Hepatology* 2006; 44:1511–1517
12. Friedrich-Rust M, Ong MF, Martens S, et al. Performance of transient elastography for the staging of liver fibrosis: a meta-analysis. *Gastroenterology* 2008; 134:960–974
13. Fraquelli M, Rigamonti C, Casazza G, et al. Reproducibility of transient elastography in the evaluation of liver fibrosis in patients with chronic liver disease. *Gut* 2007; 56:968–973
14. Coco B, Oliveri F, Maina AM, et al. Transient elastography: a new surrogate marker of liver fibrosis influenced by major changes of aminotransferases. *J Viral Hepat* 2007; 14:360–369
15. Foucher J, Castera L, Bernard PH, et al. Prevalence and factors associated with failure of liver stiffness measurement using FibroScan in a prospective study of 2114 examinations. *Eur J Gastroenterol Hepatol* 2006; 18:411–412
16. Friedrich-Rust M, Ong MF, Herrmann E, et al. Real-time elastography for noninvasive assessment of liver fibrosis in chronic viral hepatitis. *AJR* 2007; 188:758–764
17. Wai CT, Greenson JK, Fontana RJ, et al. A simple noninvasive index can predict both significant fibrosis and cirrhosis in patients with chronic hepatitis C. *Hepatology* 2003; 38:518–526
18. Bedossa P, Poynard T. An algorithm for grading of activity in chronic hepatitis C. *Hepatology* 1996; 24:289–293
19. Kondo Y, Yoshida H, Shiina S, Tateishi R, Teratani T, Omata M. Artificial ascites technique for percutaneous radiofrequency ablation of liver cancer adjacent to the gastrointestinal tract. *Br J Surg* 2006; 93:1277–1282
20. Uehara T, Hirooka M, Ishida K. Percutaneous

ultrasound-guided radiofrequency ablation of hepatocellular carcinoma with artificially induced pleural effusion and ascites. *J Gastroenterol* 2007; 42:306–311

21. Saadeh S, Cammel G, Carey WD, Youmossi Z, Barns D, Easley K. The role of liver biopsy in chronic hepatitis C. *Hepatology* 2001; 33:196–200
22. Poynard T, Ratziu V, Bedossa P. Appropriateness of liver biopsy. *Can J Gastroenterol* 2000; 14: 543–548
23. French Metavir Cooperative Study Group. Intra-observer and interobserver variation in liver biopsy interpretation in patients with chronic hepatitis C. *Hepatology* 1994; 20:15–20
24. Afdhal NH. Diagnosing fibrosis in hepatitis C: is the pendulum swinging from biopsy to blood tests? *Hepatology* 2003; 37:972–974
25. Shiina T, Nitta N, Ueno E, Bamber JC. Real time tissue elasticity imaging using the combined autocorrelation method. *J Med Ultrasonics* 2002; 29:119–128
26. Giovannini M, Hookey L, Bories E, Pesenti C, Monges G, Delpero JR. Endoscopic ultrasound elastography: the first step towards virtual biopsy? Preliminary results in 49 patients. *Endoscopy* 2006; 38:344–348
27. Gheorghe L, Gheorghe C, Cotruta B, Carabela A. CT aspects of gastrointestinal stromal tumors: adding EUS and EUS elastography to the diagnostic tools. *J Gastrointestin Liver Dis* 2007; 16:346–347